doi

Original research paper

The *in-vitro* anticancer effects of FS48 from salivary glands of *Xenopsylla cheopis* on NCI-H460 cells via its blockage of voltage-gated K^+ channels

WEICHEN XIONG[1,2,a],

HUIZHEN FAN[1,a]

QINGYE ZENG[2]

ZHENHUI DENG[2]

GUANHUI LI[2]

WANCHENG LU[2]

BEI ZHANG[2]

SHIAN LAI[3]

XIN CHEN[1,*]

XUEQING XU[2,*]

[1] *Department of Pulmonary and Critical Care Medicine, Zhujiang Hospital, Southern Medical University, Guangzhou 510282, China*

[2] *Guangdong Provincial Key Laboratory of New Drug Screening, School of Pharmaceutical Sciences, Southern Medical University, Guangzhou 510515, China*

[3] *Department of Molecular Chemistry and Biochemistry, Faculty of Science and Engineering, Doshisha University, Kyotanabe, Kyoto 610-0394, Japan*

* Correspondence; e-mail: chen_xin1020@163.com; xu2003@smu.edu.cn

[a] These authors contribute equally to the work.

Accepted August 23, 2022

Published online August 23, 2022

ABSTRACT

Voltage-gated K^+ (K_v) channels play a role in the cellular processes of various cancer cells, including lung cancer cells. We previously identified and reported a salivary protein from the *Xenopsylla cheopis*, FS48, which exhibited inhibitory activity against K_v1.1-1.3 channels when assayed in HEK 293T cells. However, whether FS48 has an inhibitory effect on cancer cells expressing K_v channels is unclear. The present study aims to reveal the effects of FS48 on the K_v channels and the NCI-H460 human lung cancer cells through patch clamp, MTT, wound healing, transwell, gelatinase zymography, qRT-PCR and WB assays. The results demonstrated that FS48 can be effective in suppressing the K_v currents, migration, and invasion of NCI-H460 cells in a dose-dependent manner, despite the failure to inhibit the proliferation. Moreover, the expression of K_v1.1 and K_v1.3 mRNA and protein were found to be significantly reduced. Finally, FS48 decreases the mRNA level of MMP-9 while increasing TIMP-1 mRNA level. The present study highlights for the first time that blood-sucking arthropod saliva-derived protein can inhibit the physiological activities of tumor cells via the K_v channels. Furthermore, FS48 can be taken as a hit compound against the tumor cells expressing K_v channels.

Keywords: lung cancer; K_v channels; FS48; NCI-H460 cells; anticancer

As a type of ion channel commonly expressed in cells, voltage-gated K^+ (K_v) channels play a critical role in the process of cellular signal transmission for both excited cells and non-excited cells, like Ca^{2+} signal transmission, action potential repolarization, hormone secretion, and cell volume regulation (1–3). Due to their significance to the above-mentioned physiological processes, K_v channels provide an ideal target for the development of some new therapeutic drugs related to anti-cancer, autoimmune, neurological, metabolic, and cardiovascular diseases.

Lung cancer is currently the malignant tumor with the highest morbidity and mortality around of the world, non-small cell lung cancer (NSCLC) in particular has been the main cancer kind globally and caused the death of more than 1.7 million annually (4, 5). The metastasis of lung carcinoma to important organs like bone, brain, lung, and liver greatly contributes to the high cancer mortality and its crucial steps include cell migration and invasion (6–9). Thus, their suppression is a matter of importance for the treatment of NSCLC. Despite significant progress made in recent years regarding the targeted drugs intended for the treatment of lung cancer, there are still no effective treatment drugs available for most patients with advanced lung cancer, especially those with metastatic advanced lung cancer (10–13). More and more studies have shown that ion channels are closely related to the proliferation, migration and metastasis of cancer and have key roles in multiple signaling pathways (14). For example, voltage-gated sodium channels (VGSCs) can enhance extracellular matrix (ECM) degradation and facilitate the metastasis of various carcinomas (15–18). Meanwhile, the role of K_v channels in tumor proliferation and growth has been demonstrated as applicable to a variety of cancer, including prostate cancer, colon cancer, lung cancer, and breast cancer (19–23). Therefore, regulating the activity of ion channels is one of the

viable solutions to anti-cancer treatment.

To overcome the host's defense response and feed, blood-sucking arthropods usually secret a rich mixture of pharmacologically active proteins from the glands. So far, there have been hundreds of different peptides and proteins responsible for regulating the hemostatic, immune, and inflammatory response of host animals that have been identified and extracted from the salivary glands of blood-sucking arthropods (24, 25). Some of them can produce significant anti-cancer effects, such as suppressing the proliferation of tumor cells, inducing cell apoptosis, inhibiting angiogenesis, and reducing the proliferation in endothelial cells (26). Especially, FS50, a $Na_v1.5$ channel blocking peptide from salivary glands of *Xenopsylla cheopis* has been reported to inhibit the motility of MDA-MB-231 human breast cancer cells via suppressing $Na_v1.5$ channel (27). In previous studies, we identified a potassium channel inhibitor, FS48, from the salivary gland of *X. cheopis*, which contains an atypical dyad motif and can dose-dependently inhibit the $K_v1.1$-1.3 channels expressed in Raw 264.7, Jurkat T and HEK 293T cells (28,29). $K_v1.1$ and $K_v1.3$ have been reported to be detected in HCI-H460 cells and are considered potential therapeutic targets (23, 30). In this study, we confirm that FS48 can inhibit the motility of NCI-H460 human lung cancer cells through the suppression of K_v currents and regulation of MMP-9 and TIMP-1 expression.

EXPERIMENTAL

Chemicals

Fetal bovine serum (FBS), RPMI-1640 medium, phosphate-buffered saline (PBS), streptomycin/penicillin, and 0.25 % trypsin-EDTA were purchased from Gibco (Waltham, MA, USA). Human lung cancer cell line NCI-H460 was purchased from CTCC (Hangzhou China) and cultured at

37°C in a humidified 5 % CO_2 atmosphere in RPMI-1640 medium containing 10 % FBS and 1 % streptomycin/penicillin. 3-(4,5-Dimethylthiazol-2-yl)-2,5-diphenyl-tetrazolium bromide (MTT) and dimethyl sulfoxide (DMSO) were purchased from Sigma-Aldrich (USA). Primary antibodies against $K_v1.1$ and $K_v1.3$ were purchased from Alomone Labs (Israel), and β-actin was purchased from Abcam (USA). TRIzol was purchased from Life Technologies (USA).

Expression and purification FS48

FS48 was expressed and purified as described in our previous studies and finally dissolved in water and stored at –80 °C until use (28). SDS-PAGE analysis showed a protein purity greater than 95 %.

Cell viability assay

The effect of FS48 on NCI-H460 cells viability was determined by the MTT assay as reported in our previous paper (31). Briefly, NCI-H460 cells (5×10^3 cells/well) were seeded into 96-well plates and treated with 0, 2, 4, 8, or 16 μM of FS48 and incubated for 24, 48, and 72 h, respectively. Following incubation, the cells were added with 10 μL MTT solution (5 mg mL^{-1} in PBS) for another 4 h to form formazan crystals in live cells. The formed formazan crystals were dissolved in DMSO, then the absorbance was read at 570 nm by a microplate reader (Tecan, Switzerland). All experiments were repeated three times.

Cell migration assay

The *in vitro* wound healing assay was performed to investigate the effect of FS48 on cell migration activity. NCI-H460 cells were seeded at 5×10^5 cells per well into a 6-well plate and grown in serum-free medium at 37 °C. Next day cell cultures were scratched using a P200 pipette tip. And then the supernatant was removed, and the cells were washed with serum-free medium three times before were

incubated with 16 μmol L^{-1} FS48 for 24 and 48 h. Representative photographs were taken at 0, 24, and 48 h at the same position of each cell well by an inverted microscope (Zeiss, Germany), and the migration index (MI) was calculated as MI = 1 – (W_t/W_0) × 100 %, where W_t is the width of the wounds at 24 or 48 h, W_0 is the width of the wounds at 0 h.

Cell invasion assay

Cell invasion was performed with a transwell chamber (Corning, USA) as previously described by us (27). Briefly, 1 × 10^5 NCI-H460 cells were loaded into the upper chamber after incubation with 0, 2, 4, 8, and 16 μmol L^{-1} FS48 in RPMI-1640 medium without FBS for 1 h. And the lower chamber was filled with RPMI-1640 medium contains 10 % FBS. Cells were allowed to migrate for 24 or 48 h at 37 °C before fixation. The top of the transwell was cleared of cells using a cotton swab. The cells move to the lower chamber were stained with crystal violet, and photographed by an inverted microscope. The dye was solubilized from the cells using 10 % (*V*/*V*) acetic acid, and the relative absorbance was quantified using a multifunction microporous plate reader reading at 570 nm. The fraction of cell invasion inhibition was calculated by normalizing to control cells. All experiments were repeated three times.

Electrophysiological measurement

Whole-cell K_v currents of NCI-H460 cells were measured using Sutter Patch Amplifier model IPA (Sutter Instrument, USA) controlled by Igor 7 software (WaveMetrics, USA) (28). The external solution contains (in mM): 5.9 KCl, 2.2 $CaCl_2$, 137 NaCl, 10 HEPES, 1.2 $MgCl_2$, and 14 D-glucose (adjusted to pH 7.3 with KOH) and the pipette solution contains (in mmol L^{-1}): 140 KF, 4 $MgCl_2$, 1 EGTA, 2 Na_2ATP, and 10 HEPES (adjusted to pH 7.3 with KOH). K_v currents were elicited by a 100 ms depolarization to +25 mV from a holding potential of −70 mV. FS48 was dissolved in the external solution for the

electrophysiological experiments and was applied with an ALA VC3 perfusion system (ALA, USA). 20 mmol L^{-1} TEA was used as a positive control. The data points were fitted to the Boltzmann equation: $I/I_{max} = 1/[1 + \exp(V - V_{1/2})/k]$ where k is the slope factor and $V_{1/2}$ is the voltage for half-maximum activation.

Gelatinase activity assay

The modified gelatinase zymography assay was performed to analyze the activity of MMP-9 according to previous study (27). NCI-H460 cells were treated with 16 μmol L^{-1} FS48 for 24 h. The supernatant was collected and electrophoresed in a 10 % SDS-PAGE gel containing 0.1 % gelatin at 100 mV for 2 h in a non-reducing environment at 4 °C. MMP-9 was activated in gel for 16 h at 37 °C after renatured with 2.5 % Triton X-100. Gels were then fixed, stained with 0.25 % Coomassie blue G-250 and destained. Gelatinase activity was quantified using Image Quant TL software (GE Healthcare, USA). All experiments were repeated three times.

Quantitative real-time PCR (qRT-PCR)

NCI-H460 cells were seeded into the six-well plates and treated with 16 μmol L^{-1} FS48 for 24 h. Total RNA was isolated from the cultured cells with the TRIzol reagent, quantified using a Nanodrop 2000 instrument (Thermo Scientific, USA), and transcribed into cDNA using the iScript cDNA Synthesis kit (Bio-Rad, USA) according to the manufacturer's instructions. qPCR was carried out with ABI 7500 Sequencing Detection System (Applied Biosystems, USA) and SYBR premix Ex Taq (Takara, Japan) according to the manufacturer's instruction. The primer sequences used for qPCR were listed as follow: GAPDH (forward: 5′-CGGAGTCAACGGATTTGGTCGTAT-3′; reverse: 5′-

AGCCTTCTCCATGGTGGTGAAGAC-3′); MMP-9 (forward: 5′-GACGAGGGCCTGGAGTGT-3′; reverse: 5′-TGTGCTGTAGGAAGCTCATCTC-3′); TIMP-1 (forward: 5′-ACCCCTGGAGCACGGCT-3′; reverse: 5′-CCCACCTTCCAAGTTAGTGACA-3′); $K_v1.1$ (forward: 5′-TGCAGTGTACTTTGCCGAGGCG-3′; reverse: 5′-GACACCACCGCCCACCAGAAAG-3′); $K_v1.3$ (forward: 5′-TGCGGTTCTTCGCTTGTC-3′; reverse: 5′-GTCCATTGCCCTGTCGTT-3′). Forty amplification cycles were necessary to achieve exponential amplification. All experiments were repeated three times. Products were quantified using $2^{-\Delta\Delta CT}$ method and $K_v1.1$, $K_v1.3$, MMP-9, and TIMP-1 gene expression was normalized to the fold change of GAPDH mRNA.

Western blot analysis

5×10^5 NCI-H460 cells were maintained in a 6-well plate overnight and treated with 16 μM FS48 for 24 h. The cells treated with PBS were considered as a negative control. Cells were harvested and lysed with RIPA lysis buffer containing phosphatase and protease inhibitors (FDbio, China) on ice for 8 min and then centrifuged at 14,000 rpm at 4 °C for 15 min. The supernatant was prepared for western blot analysis. Then, the denatured protein was loaded and separated using 10 % SDS-PAGE and transferred onto PVDF membranes (Millipore, USA). Membranes were blocked with 5 % skim milk for 1 h at room temperature. Primary antibodies against $K_v1.1$ and β-Actin (4 °C, 16 h, 1:1000), and horseradish peroxidase (HRP) conjugated secondary antibodies (26 °C, 2 h 1:1000) were used according to the manufacturer's instructions, respectively. Finally, fluorescent signals were visualized and captured with Kodak XAR film. All experiments were repeated three times.

Statistical analysis

All data are presented as mean ± SEM. Data analysis used two-way analysis of variance (ANOVA)

followed by Tukey's multiple comparison tests. $p < 0.05$, $p < 0.01$, or $p < 0.001$ represented statistically significant difference.

RESULTS AND DISCUSSION

FS48 suppresses the motility but not proliferation of NCI-H460 cells

The MTT assay showed that 2, 4, 8, and 16 μmol L^{-1} of FS48 did not inhibit the proliferation of NCI-H460 cells after incubation for 24, 48, and 72 h (Fig. 1a-c). In the wound healing assay, compared with the control group, FS48 suppressed the migration of NCI-H460 cells at 16 μmol L^{-1} after 24 and 48 h of treatment. In detail, untreated NCI-H460 cells accounted for about 37.3 and 52.2 % of the original wound area after 24 and 48 h, respectively (Fig. 1d,e). However, after treated with 16 μmol L^{-1} FS48 for 24 and 48 h, the cells only accounted for 9.86 and 18.20 % of the original wound area (Fig. 1e). We further used the transwell invasion experiment to verify the inhibition of FS48 on NCI-H460 cells migration. Consistent with the wound healing assay, all concentrations of FS48 (2, 4, 8, and 16 μmol L^{-1}) significantly inhibited the number of NCI-H460 cells invading through the membrane pores, and the inhibition was concentration-dependent (Fig. 1f,g).

FS48 reduces K_v currents of NCI-H460 cells

$K_v1.1$ and $K_v1.3$ channels are expressed in NCI-H460 cells (23). In addition, $K_v1.1$ channel has been reported to play an important role in cell motility of NCI-H460 cells (30). It has been proven that FS48 can inhibit the $K_v1.3$ protein expression and activity in activated Raw 264.7 and Jurkat T cells after 24 h incubation (28, 29). Therefore, the whole-cell patch clamp technique was performed to analyze the effect of FS48 on K_v currents of NCI-H460 cells. K_v currents were elicited by applying 100 ms depolarization

188 to +25 mV from a holding potential of −70 mV. After the addition of 10 μmol L^{-1} FS48, the peak K_v
189 currents in the NCI-H460 cells were reduced by about 49.56 % (Fig. 2a). A potent K_v blocker, TEA,
190 reduced K_v currents of NCI-H460 cells by 94.3 % at the concentration of 20 mmol L^{-1} (Fig. 2a). The
191 current-voltage relationships are presented in Fig. 2b. A significant decrease in current at all tested
192 voltages was observed in NCI-H460 cells by incubation with 10 μmol L^{-1} FS48 or 20 mmol L^{-1} TEA.
193 Given the involvement of K_v channels in the modulation of several cells migration, blocking the K_v
194 channels can suppress cell migration, rather than cell proliferation, consistent with the results that FS48
195 inhibited NCI-H460 cells migration without affecting proliferation (32–35).

196 *FS48 inhibits the K_v1.1 and K_v1.3 expression in NCI-H460 cells*

197 Western blot experiment was performed to evaluate the effect of FS48 on K_v1.1 protein expression
198 in NCI-H460 cells. The K_v1.1 and K_v1.3 protein expression in NCI-H460 cells was reduced by 21.6 and
199 37.4 %, respectively after treated with 16 μmol L^{-1} FS48 for 24 h in comparison with untreated cells (Fig.
200 3a,b). qRT-PCR experiment was furthered to determine the effect of FS48 on the K_v1.1 and K_v1.3 mRNA
201 level. Consistently, the K_v1.1 and K_v1.3 mRNA content in NCI-H460 cells decreased by 72.0 % and
202 66.0 % after treatment with FS48 for 24 h when compared with the control group (Fig. 3c). Together,
203 these results indicated that FS48 can play a significant role in suppressing K_v-dependent migration and
204 invasion for NCI-H460 cells by reducing the K_v current and K_v1.1 and K_v1.3 protein expression.

205 *FS48 decreases the mRNA levels of MMP-9 but increases TIMP-1 mRNA levels*

206 The migration and invasion of NSCLC are very important for its metastasis from the origin of
207 tumorigenesis to other body regions such as bone, brain, and spleen, which are greatly affected by matrix
208 metalloproteinases (MMPs) and their inhibitors which are essential in tissue remodeling and ECM

degradation. Thus, their suppression is indispensable for the treatment of NSCLC (4, 6). In the gelatinase zymography assay, the activity of MMP-9 was significantly reduced by about 46.0 % in NCI-H460 cells after treated with 16 μmol L^{-1} FS48 for 24 h when compared with the control group (Fig. 4a,b). Consistently, 16 μmol L^{-1} FS48 significantly decreased the mRNA expression of MMP-9 but upregulated TIMP-1, a natural inhibitor of MMPs, when compared with the control group in NCI-H460 cells (Fig. 4c). Thus, the reduced motility of NCI-H460 cells resulted from the decrease of MMP-9 and the increase of TIPM-1 in FS48-treated cells. It is well known that modulation of MAPK/NF-κB signaling pathways are involved in the expression regulation of MMPs in NSCLC cells (36, 37). Our previous study showed that FS48 can block K_v channels and subsequently inactivate the MAPK/NF-κB pathways in activated Raw 264.7 and Jurkat T cells (28, 29). Since FS48 can inhibit the K_v currents in NCI-H460 cells, it is reasonable to assume that FS48 inhibits the mobility of NCI-H460 cells via its blockage of K_v channels and the subsequently inactivation of the MAPK/NF-κB pathways which finally regulate the expression of MMP-9 and TIMP-1.

As one of the most effective treatment solutions to lung cancer currently, chemotherapy is frequently combined with other drugs targeting different pathways in order to overcome their severe side effects and drug resistance. $K_v1.1$ channel has been proven to be a potential target against various cancer and address the resistance of tyrosine kinase inhibitors in NSCLC. FS48 has no impact on the proliferation of NCI-H460 cells but inhibits the invasion and metastasis of the cells to a significant extent. Expasy shows that as a protein with only 56 amino acids, FS48 has a small molecular weight (6 kD), a theoretical isoelectric point of 8.83 and a grand average of hydropathicity (GRAVY) of –0.566, indicating that it is well soluble in water. The plasma half-life time of FS48 was about 353.1 min, which was significantly better than that of MgTx, which is also a Kv channel inhibitor (29). The above results suggest that FS48

can be combined with other drugs such as small molecule antimetabolites, immunotherapy, endocrine therapy, alkylating agents, and anti-mitotic inhibitors (38). Since these inhibitors have displayed cytotoxic effects on lung cancer cells, it is theoretically viable for the combined treatment with FS48 to produce better synergistic and therapeutic effects. Therefore, it is necessary to conduct further studies on the combined effect of FS48 and other anti-cancer drugs to fully understand the role of FS48 in combination therapy.

CONCLUSIONS

Our study shows that FS48 blocks functional K_v channels activity in the NCI-H460 cell model of lung cancer by inhibiting the expression and activity of $K_v1.1$ and $K_v1.3$ channels and reducing cell migration and invasion by reducing MMP-9 activity. Therefore, it is demonstrated in this study for the first time that blood-sucking arthropod saliva-derived protein can play a role in inhibiting lung cancer cell motility through blocking the K_v currents and channel protein expression. In addition, a new hit molecule is identified in this study for the development of lung cancer metastasis drugs.

Acknowledgments. – The authors are very grateful for the financial support.

Conflicts of interest. – The authors declare no conflict of interest.

Funding. – The work was supported by the National Natural Science Foundation of China (grant numbers 31861143050, 31772476, and 31911530077 to X.X. and grant number 82070038 to X.C.).

Authors contributions. – Conceptualization, X.C. and X.X.; methodology, H.F. and Q.Z.; investigation, W.X., Z.D., G.L., and W.L.; analysis, B.Z. and S.L.; writing, original draft preparation, W.X. and Q.Z.; writing, review, and editing, H.F., X.C., and X.X. All authors have read and agreed to the published version of the manuscript.

REFERENCES

1. H. Wulff, N. A. Castle and L. A. Pardo, Voltage-gated potassium channels as therapeutic targets, *Nat. Rev. Drug Discov.* **8** (2009) 982–1001; https://doi.org/10.1038/nrd2983

2. M. Bachmann, W. Li, M. J. Edwards, S. A. Ahmad, S. Patel, I. Szabo and E. Gulbins, Voltage-Gated Potassium Channels as Regulators of Cell Death, *Front. Cell Dev. Biol.* **8** (2020); https://doi.org/10.3389/fcell.2020.611853

3. C. Ashton, S. K. Rhie, J. D. Carmichael and G. Zada, Role of KCNAB2 expression in modulating hormone secretion in somatotroph pituitary adenoma, *J. Neurosurg.* **134**(3) (2020) 1–7; https://doi.org/10.3171/2019.12.JNS192435

4. R. S. Herbst, D. Morgensztern and C. Boshoff, The biology and management of non-small cell lung cancer, *Nature* **553** (2018) 446–454; https://doi.org/10.1038/nature25183

5. M. Lu and Y. Su, Immunotherapy in non-small cell lung cancer: The past, the present, and the future, *Thorac. Cancer* **10**(4) (2019) 585–586; https://doi.org/10.1111/1759-7714.13012

6. P. Friedl and K. Wolf, Tumour-cell invasion and migration: diversity and escape mechanisms, *Nat. Rev. Cancer* **3** (2003) 362–374; https://doi.org/10.1038/nrc1075

7. R. R. Langley and I. J. Fidler, The seed and soil hypothesis revisited-The role of tumor-stroma interactions in metastasis to different organs, *Int. J. Cancer* **128**(11) (2011) 2527–2535; https://doi.org/10.1002/ijc.26031

8. L. L. Chen, N. Blumm, N. A. Christakis, A.-L. Barabási and T. S. Deisboeck, Cancer metastasis networks and the prediction of progression patterns, *Br. J. Cancer* **101** (2009) 749–758;

https://doi.org/10.1038/sj.bjc.6605214

9. K. Ganesh and J. Massagué, Targeting metastatic cancer, *Nat. Med.* **27** (2021) 34–44; https://doi.org/10.1038/s41591-020-01195-4

10. R. L. Siegel, K. D. Miller and A. Jemal, Cancer statistics, 2020, *CA. Cancer J. Clin.* **70**(1) (2020) 7–30; https://doi.org/10.3322/caac.21590

11. Y. Zhao and A. A. Adjei, New strategies to develop new medications for lung cancer and metastasis, *Cancer Metastasis Rev.* **34** (2015) 265–275; https://doi.org/10.1007/s10555-015-9553-5

12. H. H. Popper, Progression and metastasis of lung cancer, *Cancer Metastasis Rev.* **35** (2016) 75–91; https://doi.org/10.1007/s10555-016-9618-0

13. S. Kakiuchi, Y. Daigo, T. Tsunoda, S. Yano, S. Sone and Y. Nakamura, Genome-wide analysis of organ-preferential metastasis of human small cell lung cancer in mice., *Mol. Cancer Res.* **1** (2003) 485–99.; Retrieved from http://www.ncbi.nlm.nih.gov/pubmed/12754296

14. L. Zhang, S. Bing, M. Dong, X. Lu and Y. Xiong, Targeting ion channels for the treatment of lung cancer, *Biochim. Biophys. Acta - Rev. Cancer* **1876** (2021) 188629; https://doi.org/10.1016/j.bbcan.2021.188629

15. S. Roger, M. Potier, C. Vandier, P. Besson and J.-Y. Le Guennec, Voltage-Gated Sodium Channels: New Targets in Cancer Therapy?, *Curr. Pharm. Des.* **12** (2006) 3681–3695; https://doi.org/10.2174/138161206778522047

16. S. Roger, J. Rollin, A. Barascu, P. Besson, P.-I. Raynal, S. Iochmann, M. Lei, P. Bougnoux, Y. Gruel and J.-Y. Le Guennec, Voltage-gated sodium channels potentiate the invasive capacities of human

non-small-cell lung cancer cell lines, *Int. J. Biochem. Cell Biol.* **39** (2007) 774–786; https://doi.org/10.1016/j.biocel.2006.12.007

17. L. Gillet, S. Roger, P. Besson, F. Lecaille, J. Gore, P. Bougnoux, G. Lalmanach and J.-Y. Le Guennec, Voltage-gated Sodium Channel Activity Promotes Cysteine Cathepsin-dependent Invasiveness and Colony Growth of Human Cancer Cells, *J. Biol. Chem.* **284** (2009) 8680–8691; https://doi.org/10.1074/jbc.M806891200

18. L. Brisson, V. Driffort, L. Benoist, M. Poet, L. Counillon, E. Antelmi, R. Rubino, P. Besson, F. Labbal, S. Chevalier, S. J. Reshkin, J. Gore and S. Roger, NaV1.5 sodium channels allosterically regulate the NHE-1 exchanger and promote breast cancer cell invadopodial activity, *J. Cell Sci.* **126** (2013) 4835–42; https://doi.org/10.1242/jcs.123901

19. L. WC Chow, K.-S. Cheng, K.-L. Wong and Y.-M. Leung, Voltage-gated K+ channels promote BT-474 breast cancer cell migration, *Chinese J. Cancer Res.* **30** (2018) 613–622; https://doi.org/10.21147/j.issn.1000-9604.2018.06.06

20. H. W. Park, M. S. Song, H. J. Sim, P. D. Ryu and S. Y. Lee, The role of the voltage-gated potassium channel, Kv2.1 in prostate cancer cell migration, *BMB Rep.* **54** (2021) 130–135; https://doi.org/10.5483/BMBRep.2021.54.2.210

21. D. Aissaoui, S. Mlayah-Bellalouna, J. Jebali, Z. Abdelkafi-Koubaa, S. Souid, W. Moslah, H. Othman, J. Luis, M. ElAyeb, N. Marrakchi, K. Essafi-Benkhadir and N. Srairi-Abid, Functional role of Kv1.1 and Kv1.3 channels in the neoplastic progression steps of three cancer cell lines, elucidated by scorpion peptides, *Int. J. Biol. Macromol.* **111** (2018) 1146–1155; https://doi.org/10.1016/j.ijbiomac.2018.01.144

22. M. Spitzner, J. Ousingsawat, K. Scheidt, K. Kunzelmann and R. Schreiber, Voltage-gated K channels support proliferation of colonic carcinoma cells, *FASEB J.* **21** (2007) 35–44; https://doi.org/10.1096/fj.06-6200com

23. S. Y. Choi, H.-R. Kim, P. D. Ryu and S. Y. Lee, Regulation of voltage-gated potassium channels attenuates resistance of side-population cells to gefitinib in the human lung cancer cell line NCI-H460, *BMC Pharmacol. Toxicol.* **18** (2017) 14; https://doi.org/10.1186/s40360-017-0118-9

24. B. J. Mans, Evolution of Vertebrate Hemostatic and Inflammatory Control Mechanisms in Blood-Feeding Arthropods, *J. Innate Immun.* **3** (2011) 41–51; https://doi.org/10.1159/000321599

25. J. M. C. Ribeiro and B. Arcà, Chapter 2 From Sialomes to the Sialoverse, *Adv. In Insect Phys.* (pp. 59–118); https://doi.org/10.1016/S0065-2806(09)37002-2

26. A. C. P. Sousa, M. P. J. Szabó, C. J. F. Oliveira and M. J. B. Silva, Exploring the anti-tumoral effects of tick saliva and derived components, *Toxicon* **102** (2015) 69–73; https://doi.org/10.1016/j.toxicon.2015.06.001

27. B. Zhang, Z. Deng, B. Zeng, S. Yang, X. Chen, X. Xu and J. Wu, In-vitro effects of the FS50 protein from salivary glands of Xenopsylla cheopis on voltage-gated sodium channel activity and motility of MDA-MB-231 human breast cancer cells, *Anticancer. Drugs* **29** (2018) 880–889; https://doi.org/10.1097/CAD.0000000000000662

28. Z. Deng, Q. Zeng, J. Tang, B. Zhang, J. Chai, J. F. Andersen, X. Chen and X. Xu, Anti-inflammatory effects of FS48, the first potassium channel inhibitor from the salivary glands of the flea Xenopsylla cheopis, *J. Biol. Chem.* **296** (2021) 100670; https://doi.org/10.1016/j.jbc.2021.100670

29. Q. Zeng, W. Lu, Z. Deng, B. Zhang, J. Wu, J. Chai, X. Chen and X. Xu, The toxin mimic FS48 from the salivary gland of Xenopsylla cheopis functions as a Kv1.3 channel-blocking immunomodulator of T cell activation, *J. Biol. Chem.* **298** (2022) 101497; https://doi.org/10.1016/j.jbc.2021.101497

30. W. Il Jeon, P. D. Ryu and S. Y. Lee, Effects of voltage-gated K+ channel blockers in gefitinib-resistant H460 non-small cell lung cancer cells., *Anticancer Res.* **32** (2012) 5279–84.; Retrieved from http://www.ncbi.nlm.nih.gov/pubmed/23225427

31. J. Wu, H. Zhang, X. Chen, J. Chai, Y. Hu, W. Xiong, W. Lu, M. Tian, X. Chen and X. Xu, FM-CATH, A Novel Cathelicidin From Fejervarya Multistriata, Shows Therapeutic Potential for Treatment of CLP-Induced Sepsis, *Front. Pharmacol.* **12** (2021); https://doi.org/10.3389/fphar.2021.731056

32. M. Song, S. Park, J. Park, J. Byun, H. Jin, S. Seo, P. Ryu and S. Lee, Kv3.1 and Kv3.4, Are Involved in Cancer Cell Migration and Invasion, *Int. J. Mol. Sci.* **19** (2018) 1061; https://doi.org/10.3390/ijms19041061

33. K. Silver, A. Littlejohn, L. Thomas, E. Marsh and J. D. Lillich, Inhibition of Kv channel expression by NSAIDs depolarizes membrane potential and inhibits cell migration by disrupting calpain signaling, *Biochem. Pharmacol.* **98** (2015) 614–628; https://doi.org/10.1016/j.bcp.2015.10.017

34. W. K. K. Wu, G. R. Li, T. M. Wong, J. Y. Wang, L. Yu and C. H. Cho, Involvement of voltage-gated K+ and Na+ channels in gastric epithelial cell migration, *Mol. Cell. Biochem.* **308** (2008) 219–226; https://doi.org/10.1007/s11010-007-9631-2

35. J. N. Rao, O. Platoshyn, L. Li, X. Guo, V. A. Golovina, J. X. J. Yuan and J.-Y. Wang, Activation of K + channels and increased migration of differentiated intestinal epithelial cells after wounding,

Am. J. Physiol. Physiol. **282** (2002) C885–C898; https://doi.org/10.1152/ajpcell.00361.2001

36. S.-H. Wu, Y.-T. Hsiao, C.-L. Kuo, F.-S. Yu, S.-C. Hsu, P.-P. Wu, J.-C. Chen, T.-C. Hsia, H.-C. Liu, W.-H. Hsu and J.-G. Chung, Bufalin Inhibits NCI-H460 Human Lung Cancer Cell Metastasis In Vitro by Inhibiting MAPKs, MMPs, and NF-κB Pathways, *Am. J. Chin. Med.* **43** (2015) 1247–1264; https://doi.org/10.1142/S0192415X15500718

37. J. H. Kim, E. B. Cho, J. Lee, O. Jung, B. J. Ryu, S. H. Kim, J. Y. Cho, C. Ryou and S. Y. Lee, Emetine inhibits migration and invasion of human non-small-cell lung cancer cells via regulation of ERK and p38 signaling pathways, *Chem. Biol. Interact.* **242** (2015) 25–33; https://doi.org/10.1016/j.cbi.2015.08.014

38. C. Zhang, N. B. Leighl, Y.-L. Wu and W.-Z. Zhong, Emerging therapies for non-small cell lung cancer, *J. Hematol. Oncol.* **12** (2019) 45; https://doi.org/10.1186/s13045-019-0731-8

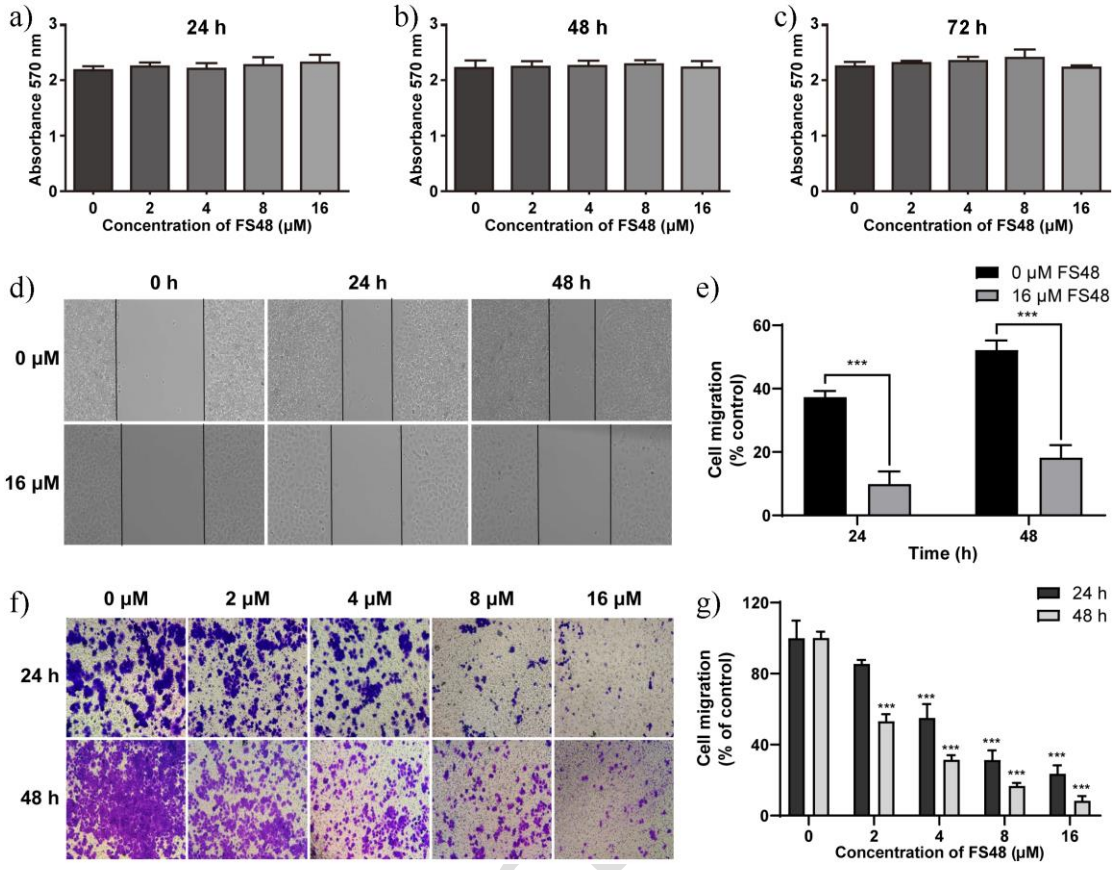

Fig. 1. Effects of FS48 on the proliferation and mobility of NCI-H460 cells. a-c) Effects of FS48 on the proliferation of NCI-H460 cells. NCI-H460 cells were treated with indicated concentrations of FS48 and incubated for 24, 48, and 72 h before its proliferations were assessed by MTT; d) wound healing assay; e) statistical analysis for wound healing assay; f) transwell invasion assay; g) statistical analysis for wound healing assay. Data are represented as mean ± SEM ($n = 3$). ***$p < 0.001$ compared with control.

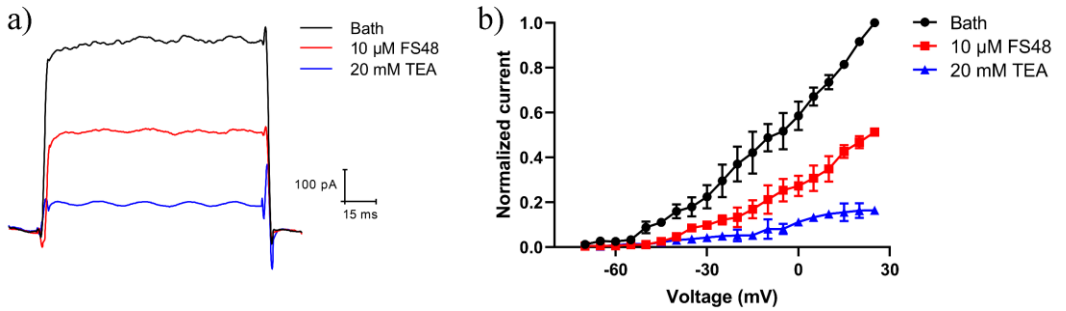

376

377

378 Fig. 2. Effects of FS48 on K_v currents in NCI-H460 cells. a) Representative K^+ currents recorded in NCI-

379 H460 cells before and after perfusion with 10 μmol L^{-1} FS48 or 20 mmol L^{-1} TEA. Currents were evoked

380 by 100 ms voltage steps from a holding potential of −70 mV to +25 mV; b) current-voltage relationships

381 (−70 to +25 mV at 5 mV intervals). Data are represented as mean ± SEM (n = 3).

382

383

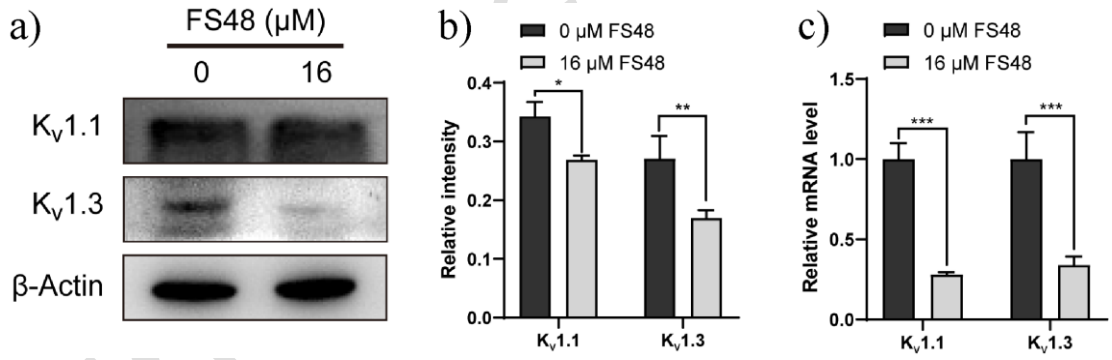

384

385 Fig. 3. Effects of FS48 on K_v1.1 and K_v1.3 expression. a) Expression of K_v1.1 and K_v1.3 in NCI-H460

386 cells after 24 h incubation with FS48 was analyzed with Western blot; b) quantitative analysis of Western

387 blot; c) effect of FS48 on relative K_v1.1 and K_v1.3 mRNA levels in NCI-H460 cells. Data are represented

388 as mean ± SEM (n = 3). *p < 0.05, **p < 0.01, and ***p < 0.001 compared with control.

389

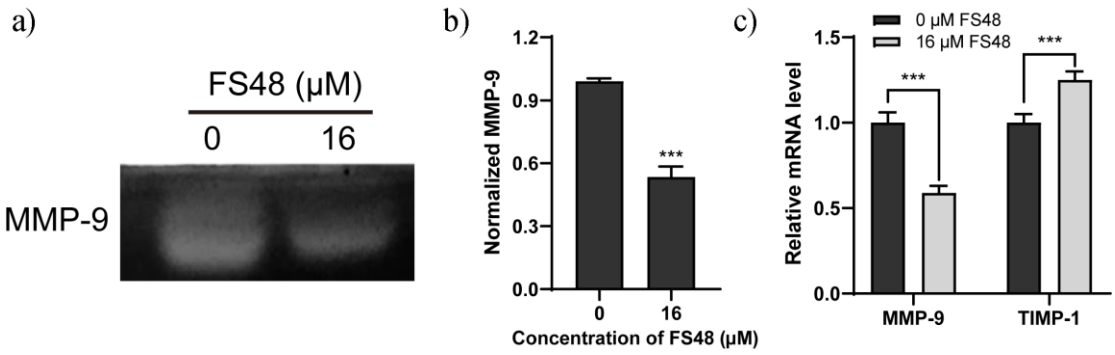

Fig. 4. The expression changes of MMP-9 and TIMP-1 in NCI-H460 cells. a) Gelatinase activities for band densities of MMP-9 from HCI-H460 cells treated with FS48 for 24 h; b) quantitation of gelatinase zymogram; c) effect of FS48 on relative MMP-9 and TIMP-1 mRNA levels in NCI-H460 cells. Data are represented as mean ± SEM (n = 3). ***p < 0.001 compared with control.